Journal of Water Process Engineering 78 (2025) 108721

Contents lists available at ScienceDirect

Journal of Water Process Engineering

journal homepage: www.elsevier.com/locate/jwpe

Influence of temperature and dissolved oxygen on nitrification in a membrane bioreactor treating urine☆

Weonjung Sohn [a], Andrea Merenda [a], A.H. Shafaghat [a], Ibrahim El Saliby [a], Ying Zhang [b], Xiaodong Jia [b], Jing Guan [b], Sherub Phuntsho [a], Ho Kyong Shon [a,*]

[a] ARC Industry Hub for Nutrients in a Circular Economy (ARC NiCE Hub), Centre for Technology in Water and Wastewater, School of Civil and Environmental Engineering, University of Technology Sydney (UTS), City Campus, 15 Broadway, NSW, 2007, Australia

[b] Beijing Origin Water Membrane Technology Company Ltd., Beijing, 101400, China

ARTICLE INFO

Guest Editors: Soraya Malinga
Overseeing Editor: Ludovic F. Dumee

Keywords:
Source-separated urine
Biological nitrification
Membrane bioreactor
Temperature
Dissolved oxygen

ABSTRACT

The biological nitrification of source-separated urine in a membrane bioreactor (MBR) is recognised as a promising approach to transform it into liquid fertiliser. However, a major limitation is the prolonged hydraulic retention time (HRT), which increases the system footprint. Given the strong dependence of nitrification on temperature and dissolved oxygen (DO) conditions, this study investigated the effects of three different temperatures (10 °C, 20 °C, and 30 °C) and DO levels (2, 4, and 6 mg/L) to determine the optimal conditions for enhanced nitrification performance and the resulting minimised HRT. Concurrently, microbial analysis was conducted to gain a comprehensive understanding of the MBR system. Results indicated that high DO levels resulted in poor biomass growth and a higher abundance of ammonia-oxidising bacteria (AOB) compared to the nitrite-oxidising bacteria (NOB), *Nitrospira*. At 10 °C, *Nitrosomonas*, was more prevalent than *Nitrosococcus* as an AOB. Conversely, at 30 °C, the relative abundance of *Nitrosococcus* increased by up to three-fold, leading to higher nitrite concentrations. Overall, the optimal conditions were found to be a temperature of 20 °C and a DO level of 4 mg/L, achieving a nitrification rate of 201 ± 49 mgN/L·d and the shortest HRT of 8 ± 2 days, with *Nitrosococcus* and *Nitrospira* as the predominant AOB and NOB, respectively. The findings suggest that optimising DO at moderate temperatures enhances nitrification while reducing aeration energy. These results inform energy-efficient operational strategies for decentralised nutrient recovery systems from human urine.

1. Introduction

As global food production increases and dependence on fertilisers grow, human urine, typically considered waste, has significant potential as a substantial nutrient source when properly separated. The key challenges of the direct agricultural use of urine, such as unpleasant odours, high organic content, and ammonia volatilisation due to high pH, have led to increased attention on various urine treatment technologies. Among these, the biological nitrification in ultrafiltration membrane bioreactors (UF-MBR) has emerged as an effective solution for stabilising ammonia and removing malodourous organics. Compared to other reactor configurations, such as sequencing batch reactors (SBRs), fluidised bed reactors (FBRs), or continuous stirred-tank reactors (CSTRs), MBRs offer distinct advantages by retaining biomass via membrane separation, thereby enabling longer sludge retention times, which is particularly beneficial for sustaining slow-growing nitrifying bacteria, despite their higher capital costs. Treating urine in an MBR process yields a safe and odourless liquid fertiliser, facilitating the complete recovery of key nutrients [1,2]. This highlights the essential role of biological nitrification in urine as a fundamental aspect of resource recovery, emphasising its importance in the sustainable management of vital nutrients.

In the MBR system, while heterotrophic bacteria effectively remove the high organic matters, nitrification, carried out by autotrophic nitrifying bacteria transforms ammonia into nitrate, which can lower pH levels by consuming alkalinity, without requiring chemical additives [3,4]. Ammonia-oxidising bacteria (AOB) firstly oxidises ammonia into nitrite, and then nitrite-oxidising bacteria (NOB) oxidises nitrite into nitrate. The composition of AOB and NOB populations can fluctuate based on environmental factors like substrate availability and salinity

☆ This article is part of a Special issue entitled: 'Trailblazer 2024' published in Journal of Water Process Engineering.

* Corresponding author.
E-mail address: Hokyong.Shon-1@uts.edu.au (H.K. Shon).

https://doi.org/10.1016/j.jwpe.2025.108721
Received 6 June 2025; Received in revised form 4 September 2025; Accepted 7 September 2025
Available online 15 September 2025
2214-7144/

[5,6]. If NOB activity lags behind AOB, nitrite accumulation may occur, potentially harming both bacterial groups [7–9]. As such, maintaining a balanced oxidation rate between these groups is vital for stable nitrification, but this balance is influenced by temperature, dissolved oxygen (DO), and pH levels [10].

Previous lab-scale studies on urine-treating MBRs have typically been conducted at a controlled pH of 6.2, selected to minimise nitrite accumulation while balancing the activity of AOB and NOB [3]. However, these systems were primarily tested under room temperature conditions (21 °C) and at a constant DO level of approximately 4–4.5 mg/L [3,10,11]. As a result, the specific effects of temperature and DO on the nitrification of urine remain largely unexplored, to the best of our knowledge. Given the importance of these parameters, many studies have focused on their impact on biological nitrification, including the kinetics of AOB and NOB, in the treatment of various types of wastewater. The different temperature responses of AOB and NOB can lead to imbalances in the nitrification process under varying temperature conditions. Previous studies have reported that at temperatures below 16 °C, the growth rate of NOB (around 0.6 d^{-1}) slightly exceeds that of AOB (around 0.5 d^{-1}), whereas at higher temperatures, the growth rate of AOB increases exponentially compared to NOB [12,13]. Other studies have consistently reported that AOB showed higher abundance at 30 °C compared to 10 °C, whereas NOB had greater tolerance at lower temperature conditions between 10 °C and 15 °C [14,15]. This suggests that stable nitrification with minimal nitrite accumulation is more feasible at lower temperatures. Conversely, at higher temperatures, nitrite accumulation can occur due to the imbalance in oxidation rates between AOB and NOB. Therefore, maintaining an optimal temperature range is essential for effective and stable nitrification. Furthermore, nitrifying bacteria rely on oxygen as an electron acceptor, making their growth and activity highly dependent on adequate DO levels. It was reported that the growth rates of nitrifiers begin to decline at DO concentrations below 3–4 mg/L or higher of this level, with significant reductions observed below 2 mg/L [16]. Another study suggested that DO concentrations above 6 mg/L could significantly enhance the AOB activity while strongly inhibiting NOB [17]. In addition, several studies have concluded that AOB can dominate under low DO conditions due to their higher oxygen affinity than NOB [18,19]. However, some studies have reported contrasting results, indicating that certain NOB, particularly *Nitrospira,* possess a higher oxygen affinity than AOB, enabling them to adapt well to low DO environments [20,21]. As such, further investigation is necessary to better understand and manage these dynamics for optimising nitrification processes.

This study provides novel insights into optimising urine nitrification in MBRs by systematically exploring how temperature and DO concentrations affect both nitrification performance and microbial community structure. These are critical operational parameters that significantly influence nitrification efficiency, hydraulic retention time (HRT), and overall system energy consumption. While previous studies have examined urine treatment in MBRs under standard room temperature and DO conditions, the specific interactions between these two parameters and their influence on both nitrification kinetics and microbial community composition have not been explored in detail. This work addresses this knowledge gap by identifying the optimal operational conditions that maximise nitrification efficiency while minimising energy consumption. Furthermore, high-throughput microbial community sequencing reveals, for the first time, temperature-dependent shifts in the dominant AOB and NOB. The specific objectives are: (1) to evaluate nitrification efficiency under varying temperature and DO conditions; (2) to assess changes in the microbial community using high-throughput sequencing; and (3) to identify optimal operational parameters for energy-efficient and stable nitrification. It was hypothesised that an optimal combination of temperature and DO would maximise nitrification efficiency and minimise HRT in urine-treating MBRs, and that these operational conditions would be reflected in distinct shifts in the balance between AOB and NOB. The results aimed to support the design of decentralised, energy-efficient nutrient recovery systems using MBR technology for urine treatment.

2. Materials and methods

2.1. Urine collection and seed sludge

Building 11 at the University of Technology Sydney (UTS) is equipped with urine-diverting infrastructure, including waterless urinals connected to dedicated urine collection pipes installed on each floor. The collected urine was stored in a 100 L water tank located in the basement. For the operation of lab-scale MBR, the stored urine was transferred from the basement tank whenever feed urine was required. The carbon to nitrogen to phosphorous (C:N:P) ratios were maintained at approximately 3.8:14.5:1. The detailed composition of the feed urine is presented in Table 1. As the urine used in this study was fully hydrolysed in the storage tank prior to feeding, urea was no longer present, and the reported concentrations directly represent the natural composition of the collected source-separated urine without any adjustment. The seed sludge used in this study was obtained from a Central Park decentralised wastewater treatment plant, Sydney Ultimo, New South Wales, Australia. The microbial community profile of the seed sludge is described in our previous work [22]. For inoculation, the sludge was systematically acclimated to urine treatment. This was achieved by initially using ten-fold diluted urine and gradually transitioning to undiluted urine, following the protocol established in the previous study [2]. The acclimation period lasted approximately two months without any sludge withdrawal. After successful adaptation to undiluted urine, the mixed liquor sludge was used to inoculate the three lab-scale MBRs in this study.

2.2. Experimental set-up

Three aerobic MBR systems, each with a 4 L working volume, were set up in double-jacketed glass reactors. A circulator was used to circulate water through the outer layer of the reactors, which were connected to each other to enable consistent water flow in the outer layer. This configuration effectively ensured constant temperature control of the reactors during the operation. This study aimed to evaluate the effects of three temperature conditions (10, 20, and 30 °C) combined with three DO levels (2, 4, and 6 mg/L), resulting in nine operational scenarios. The selected temperatures represent realistic operational conditions for decentralised urine treatment systems, ranging from colder climates (~10 °C) to standard indoor laboratory conditions (~20 °C) and warmer climates (~30 °C). These values also reflect seasonal ranges commonly encountered in Australian regions, enabling simulation of real-world scenarios [23–25]. The DO setpoints (2, 4, and 6 mg/L) were chosen based on prior literature identifying this

Table 1
Composition of source-separated urine used as feed for MBR systems.

Component (unit)	Feed urine
NH_4^+-N ($mg_N.L^{-1}$)	3460 ± 152
NO_3-N ($mg_N.L^{-1}$)	n.d.
NO_2-N ($mg_N.L^{-1}$)	n.d.
PO_4^{3-}-P ($mg_P.L^{-1}$)	238 ± 21
K^+ (mg/L)	982 ± 83
SO_4^{2-} (mg/L)	745 ± 61
Cl^- (mg/L)	2750 ± 130
Na^+ (mg/L)	1133 ± 101
Ca^{2+} (mg/L)	1 ± 0.5
Mg^{2+} (mg/L)	1.7 ± 0.5
TOC (mg/L)	905 ± 76
EC (mS cm^{-1})	26 ± 2
pH	9.3 ± 0.1

n.d.: not detected.

range as relevant for aerobic microbial processes, with 2 mg/L representing a lower oxygen threshold, 4 mg/L as the previously studied baseline, and 6 mg/L representing a higher DO condition [16,17,26]. Hollow fibre ultrafiltration (UF) membrane modules (polyvinylidene fluoride, pore size 0.02 μm, OriginWater, China) with an inner diameter of 0.55 mm, an outer diameter of 1.65 mm, and a total surface area of 0.02 m^2, were submerged in each reactor. The membrane module was operated under low transmembrane pressure conditions, maintaining a flux of up to 1 $L/m^2 \cdot h$, which contributed to the minimal membrane fouling observed in this study. The pH in the reactor was continuously monitored and controlled using a pH meter (HI6100405, Hanna Instruments, Australia) connected to a pH dosing pump (BL7916–1, Hanna Instruments, Australia). Whenever the pH level decreased due to alkalinity consumption during the nitrification process, the dosing pump automatically added high-pH urine (pH 9.2) to maintain the reactor pH at 6.2 ± 0.1. The pH control is particularly important as it determines the equilibrium between NH_4^+/NH_3 and HNO_2/NO_2^-, directly influencing the activity and kinetics of AOB and NOB. Maintaining an optimal pH not only supports balanced nitrifier activity but also prevents nitrite accumulation, which is undesirable for agricultural reuse due to its negative effects on plants [27]. While increasing pH toward neutral may enhance nitrification rates by increasing ammonia availability for AOB, it can also elevate free ammonia concentrations, which can inhibit nitrification, and may lead to greater ammonia volatilisation and nitrite accumulation resulting from NOB inhibition [28]. Accordingly, this study maintained the pH at 6.2 ± 0.1 to enable a focused assessment of temperature and DO effects. As a result, the HRT was regulated based on the urine dosing rate to stabilise the pH. In addition, no sludge was withdrawn from the system during the operational period, therefore, the sludge retention time (SRT) was effectively infinite. All reactors were aerated using ceramic air diffusers. This setup enabled the maintenance of three distinct DO concentrations across the reactors. The DO levels were set at 2.0 ± 0.1, 4.0 ± 0.1, and 6.0 ± 0.1 mg/L by individually adjusting the air flow rates for each reactor. Each MBR was referred to as R1, R2, and R3 in this study. In R1 (2 mg O_2/L), air flow rates were controlled at 0.2 ± 0.05, 0.4 ± 0.05, and 0.8 ± 0.1 L/min for 10 °C, 20 °C, and 30 °C, respectively. For R2 (4 mg O_2/L), the flow rates were 0.5 ± 0.05, 0.8 ± 0.05, and 1.2 ± 0.1 L/min. For R3 (6 mg O_2/L), air flow rates were 1.0 ± 0.1, 1.8 ± 0.1, and 3.1 ± 0.1 L/min at the respective temperature conditions. DO concentrations were continuously monitored using an optical DO meter (HI98198, Hanna Instruments, Australia). Air flow rates were adjusted manually based on real-time DO measurements to ensure stable maintenance of the target concentrations throughout the experiment. Fig. 1 shows the schematic diagram of experimental set-up.

Three parallel MBRs were operated for 120 days to evaluate the nitrification performance, the TOC removal efficiency, and the biomass growth. To assess the impact of temperature on nitrification, the reactors were sequentially adjusted to operate at 10 °C, 20 °C, and 30 °C. The inoculative sludge for this study was derived from a urine-treating MBR system acclimated to hydrolysed urine at room temperature. Accordingly, the reactors were initially adjusted to 10 °C by gradually lowering the temperature of the circulating water through the outer layer of the three reactors. This temperature condition was maintained for 30 days, after which the temperature was gradually increased to 20 °C at a rate of 1 °C per day. The 20 °C and 30 °C conditions were also maintained for 30 days each, with a 10-day transitional period between temperature adjustments. During each temperature transition period, no significant changes in the system performance were observed. Instead, the reactors demonstrated gradual adaptation, with measurable changes in performance parameters becoming evident only after the temperature had been fully adjusted and stabilised at the target value. Simultaneously, the effect of DO concentrations was investigated by operating each reactor at DO levels of 2.0 ± 0.1 mg/L (R1), 4.0 ± 0.1 mg/L (R2), and 6.0 ± 0.1 mg/L (R3).

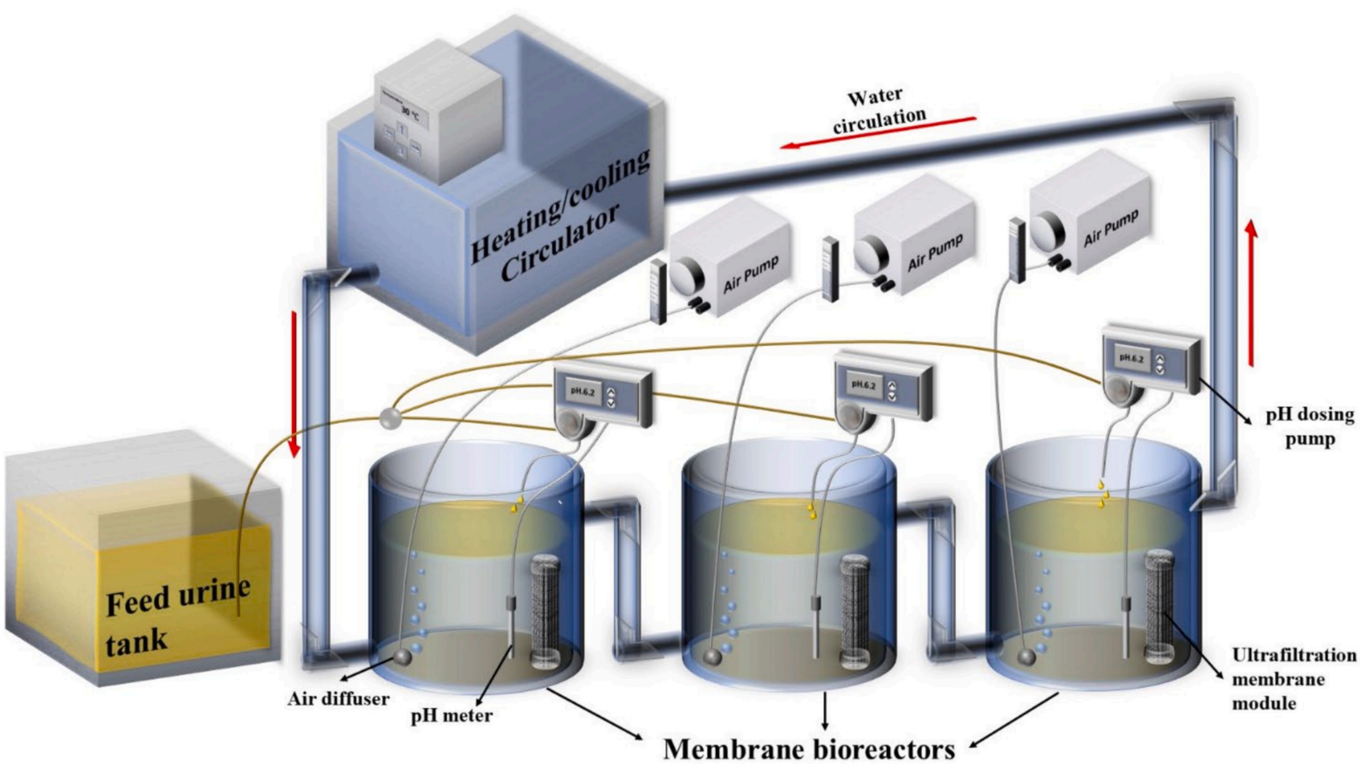

Fig. 1. Schematic diagram of the experimental set-up, which consists of a heating/cooling water circulator connected to three membrane bioreactors (MBRs), each contained within a double-layered glass reactor for temperature control.

2.3. Analytical methods

2.3.1. Nutrient, biomass, total organic carbon and data analysis

Nutrients concentrations of source-separated urine and MBR effluent were analysed using a standard test kit (Merck Millipore, Burlington, USA) and a photometer (Spectroquant NOVA 60, Merck, Germany) for anions, while cations were measured via Inductively coupled plasma mass spectrometry (ICP-MS). The concentrations of Mixed Liquor Suspended Solids (MLSS) and Mixed Liquor Volatile Suspended Solids (MLVSS) during the operational period were measured according to the standard methods. The MLVSS/MLSS ratio was also monitored as an indicator of the concentration of active microorganisms during operation. The sludge volume index (SVI) was measured by standard methods [29]. Total organic carbon (TOC) concentration was determined by a TOC analyser (Analytik Jena Multi N/C 2000).

For data analysis, the paired *t*-test analysis was carried out in Microsoft Excel to determine the statistical significance of the data obtained. Differences between average values were considered statistically significant at the 5 % level ($p \leq 0.05$).

2.3.2. Amplicon sequencing and bioinformatics analysis

The suspended sludge was sampled from each reactor at the end of nine different operational periods prior to condition transitions for the microbial community analysis. The samples were delivered to the UTS Next Generation Sequencing Facility, Sydney, Australia, for DNA extraction and amplicon sequencing. The V3-V4 regions of bacterial and archaeal 16S rRNA genes were amplified using the universal primer set Pro341F (5'-CCTAYGGGRBGCASCAG-3′) and Pro806R (5'-GGACTACNNGGGTATCTAAT-3′), to obtain a comprehensive profile of the microbial community [30]. Paired-end amplicon sequencing (2 × 300 bp) was carried out using the Illumina MiSeq platform at the UTS sequencing facility. The raw sequence data were initially processed with the Illumina bcl2fastq pipeline. The raw reads underwent microbial community and diversity analysis using on CJ Bioscience's bioinformatics cloud platform EzBioCloud with 16S-based metagenome taxonomic profiling (MTP) [31].

3. Results and discussion

3.1. Effect of temperature and DO on MBR performance

The biological nitrification process in the MBR proceeds via a two-step pathway: (1) ammonia oxidation by AOB ($NH_4^+ + 1.5\ O_2 \rightarrow NO_2^- + 2H^+ + H_2O$); and (2) nitrite oxidation by NOB ($NO_2^- + 0.5\ O_2 \rightarrow NO_3^-$). Fig. 2**a, b,** and **c** depict the nitrification performance of the reactors under varying temperature and DO conditions over the whole operational period. At 10 °C, all reactors exhibited reduced nitrification rates compared to those reported for urine MBR systems operating at room temperature, leading to increased HRTs of over 11 days. While the difference of nitrification rates between R1 and R3 was insignificant ($p > 0.05$), R2 achieved the highest nitrification rate of 162 ± 38 mgN/L·d and the shortest HRT of 11 ± 2 days at 10 °C ($p < 0.05$). As the temperature increased to 20 °C, R1 and R3 achieved HRTs of 12 ± 4 days and 15 ± 7 days, corresponding to the nitrification rates of 136 ± 45 mgN/L·d and 97 ± 30 mgN/L·d respectively ($p < 0.05$). R2 exhibited the shortest HRT of 8 ± 2 days and achieved the highest nitrification rate of

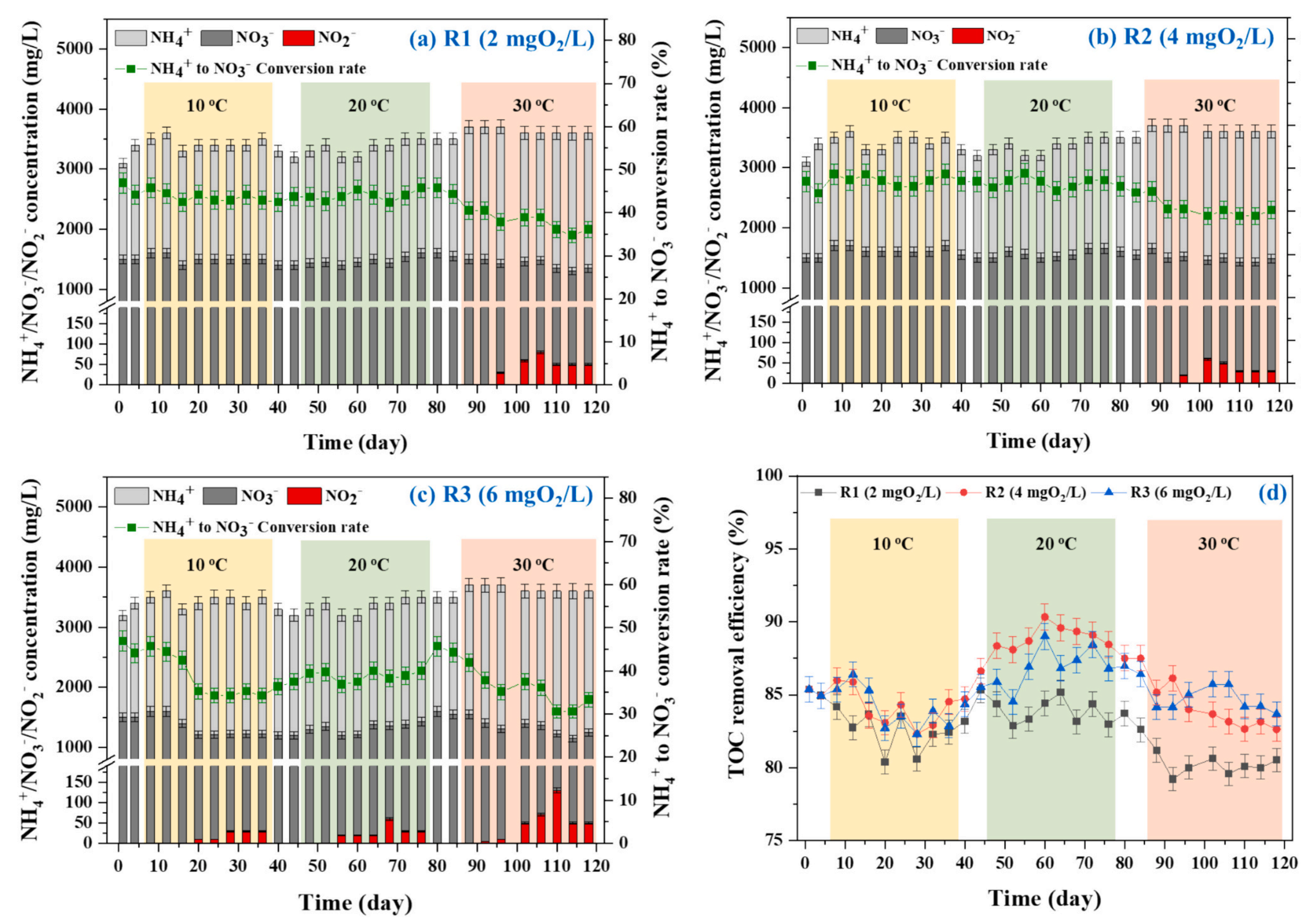

Fig. 2. Nitrification performance in terms of ammonium (NH_4^+), nitrate (NO_3^-), and nitrite (NO_2^-) concentrations (primary y-axis, left, in mgN/L) and NH_4^+ to NO_3^- conversion rate (secondary y-axis, right, in %) for (a) R1 (2 mgO_2/L); (b) R2 (4 mgO_2/L); (c) R3 (6 mgO_2/L); and (d) total organic carbon (TOC) removal efficiency (%) of the three reactors.

201 ± 49 mgN/L·d, representing the optimal performance across all operational conditions ($p < 0.05$). When compared to previous studies, the nitrification rate observed in this work is comparable to that reported by Sohn et al. (2024), where a rate of 194 ± 60 mgN/L·d and an HRT of 10 ± 3 days were achieved in a urine-treating MBR operated at room temperature with a DO level of 4.5 ± 0.1 mg/L [22]. In contrast, this study shows a marked improvement over the results of Volpin et al. (2020), who reported a nitrification rate of only 65 mgN/L·d at an HRT of approximately 20 days when operated at room temperature and DO concentrations exceeding 6 mg/L [3]. A more recent study reported higher nitrification rates of 313.9 mgN/L·d under comparable conditions, however, this outcome was achieved with nearly double the biomass concentration (10 g/L of MLVSS) and a feed urine ammonium concentration approximately one-fourth of that applied in the present study (~900 mg/L) [32]. These comparisons highlight the effectiveness of optimising both temperature and DO conditions for enhanced nitrification performance in urine MBR systems.

At 30 °C, nitrification rates declined in all reactors, which dropped to averages of 61 ± 41, 107 ± 44, and 51 ± 34 mgN/L·d for R1, R2 and R3, respectively, leading to a substantial raise in HRTs by 88–125 %. While the nitrification rates in R1 and R3 were not significantly different ($p > 0.05$), R2 maintained a significantly higher rate than the other reactors under these elevated temperature conditions ($p < 0.05$). Additionally, nitrite accumulation was observed in all reactors after 10 days of operation at this temperature condition. While R1 and R2 accumulated up to 60–80 mgN/L, R3 exhibited the highest nitrite concentration of 130 mgN/L. This is primarily due to a kinetic imbalance between AOB and NOB. At higher temperatures, AOB generally exhibit higher maximum growth rates than NOB [12]. Accordingly, microbial profiling in this study (Section 3.3.2) showed a disproportionate increase in AOB and a decline in NOB. This imbalance is consistent with prior reports that AOB exponentially outpace NOB at elevated temperatures, promoting nitrite build-up. [12,33]. Moreover, despite our controlled pH (6.2), increased nitrite elevates free nitrous acid (FNA) levels, which likely inhibited both nitrifiers and thus further limited nitrification and increased the HRT [34]. Remarkably, slight nitrite accumulation was also observed in R3 at 10 °C and 20 °C, which could be attributed to significantly promoted AOB growth under high DO conditions compared to NOB. This finding aligns with previous study which demonstrated that the high DO operation (~5 mg/L) promoted faster AOB growth, leading to its dominance within the aerobic nitrifier community compared to low DO condition (~2 mg/L). This might be due to the higher specific growth rate of AOB under sufficient oxygen-supplied environments, providing a competitive advantage in occupying habitat space [35].

In terms of TOC removal efficiency, all three reactors demonstrated excellent TOC removal efficiencies, exceeding 80 % under all temperature conditions, as shown in Fig. 2d. On day 0, the initial TOC removals were identical across all reactors, a result attributed to the use of the same acclimated seed sludge sourced from the urine-treating MBR, which provided comparable initial microbial communities and TOC degradation capacities. While the initial TOC removal in all three reactors was approximately 85 %, a subsequent decrease in temperature to 10 °C in R1 led to a significant reduction in the average TOC removal to 82 ± 1 % ($p < 0.05$). On the other hand, R2 and R3 showed no significant differences in average rate, both achieving 84 ± 2 %. The highest TOC removals were observed at 20 °C, with R2 achieving 89 ± 1 %, followed by R3 at 87 ± 1 %, and R1 at 84 ± 1 %, with significant differences ($p < 0.05$). When the temperature increased to 30 °C, all reactors experienced slight decline in the removal rates. R2 and R3 showed almost similar efficiencies at 84–85 % on average ($p > 0.05$), while R1 showed significantly less efficiency of 80 ± 1 %. Across all temperature conditions, R1 consistently exhibited the lowest TOC removals compared to R2 and R3, indicating that a DO level of 2 mg/L was less effective. According to the literature, the DO concentrations between 4 mg/L and 8 mg/L were highly favourable for the TOC removal, which aligns with the findings of this study [36,37]. This improvement might be attributed to increased production of extracellular polymeric substances (EPS) and a more effective distribution of multivalent ions, such as calcium, under high DO conditions, thereby enhancing the utilisation of organics as substrates by heterotrophic bacteria [38,39]. Overall, the optimal TOC removal of 89 % was achieved at 20 °C with a DO concentration of 4 mg/L. Table 2 shows the average performance results under different operational conditions.

Given that temperature control (refrigeration or heating) and aeration are closely linked to energy consumption, careful consideration of these factors is essential when translating laboratory findings to full-scale applications. Maintaining constant temperature, particularly through heating or cooling, requires significant energy input, especially over long-term operations. However, since this study resulted in 20 °C, approximately room temperature, as the optimal condition, additional temperature control may be unnecessary if systems are installed indoors or in climates where ambient conditions remain near this range, which is advantageous for decentralised deployment. In terms of aeration energy, a previous study using BioWin simulation for a full-scale MBR treating up to 25 m^3 of source-separated urine reported that maintaining a DO level of 6 mg/L required approximately 6 kWh/kg N for nitrification. Reducing the DO setpoint to 4 mg/L decreased the energy demand to between 3 and 4 kWh/kg N, while further reducing DO to 3 mg/L halved the energy consumption to about 3 kWh/kg N [40]. Given that 4 mg/L DO was identified as the optimal condition in this study, it implies that a 30–50 % reduction in energy consumption could be achieved at full scale compared to operation at a DO level of 6 mg/L. Therefore, operating under the optimal conditions at 20 °C and 4 mg/L DO, not only maximises nitrification and TOC removal performance in urine MBR but also offers significant potential for energy savings in full-scale urine nitrification systems. Translating these conditions into practice, however, will require careful consideration of several scale-up factors, including robust DO control to maintain stable airflow distribution in larger reactors, and passive thermal management, such as indoor siting and insulation to sustain operation near 20 °C without auxiliary heating or cooling. Such measures are essential for preserving the targeted microbial community under fluctuating environmental conditions. Overall, these results offer a practical framework for selecting operational parameters that balance performance and energy efficiency under real-world conditions. This work advances beyond previous studies by providing actionable guidance for system design and optimisation in decentralised nutrient recovery.

3.2. Effect of temperature and DO on biomass growth

To evaluate biomass growth under varying operational conditions, the initial MLSS concentrations in all reactors were uniformly adjusted to 5.8 ± 0.1 g/L before the commencement of each temperature condition. Fig. 3 presents the MLSS and MLVSS concentrations, the MLVSS/MLSS ratio, and the sludge volume index (SVI) measured at the conclusion of each operational phase. Across all temperature conditions, R1 showed the largest growth in MLSS and MLVSS concentrations during the operation at each temperature condition, with a 16–24 % increase in MLSS and an 11–22 % increase in MLVSS. However, this was

Table 2
Average performance results under different operational conditions.

Results		R1 (2 mgO_2/L)	R2 (4 mgO_2/L)	R3 (6 mgO_2/L)
Nitrification rate (mgN/L·d)	10 °C	101 ± 41	162 ± 38	77 ± 41
	20 °C	136 ± 45	201 ± 49	97 ± 30
	30 °C	61 ± 41	107 ± 44	51 ± 34
Avg. TOC removal rate (%)	10 °C	82 ± 1	84 ± 2	84 ± 2
	20 °C	84 ± 1	89 ± 1	87 ± 1
	30 °C	80 ± 1	84 ± 1	85 ± 1

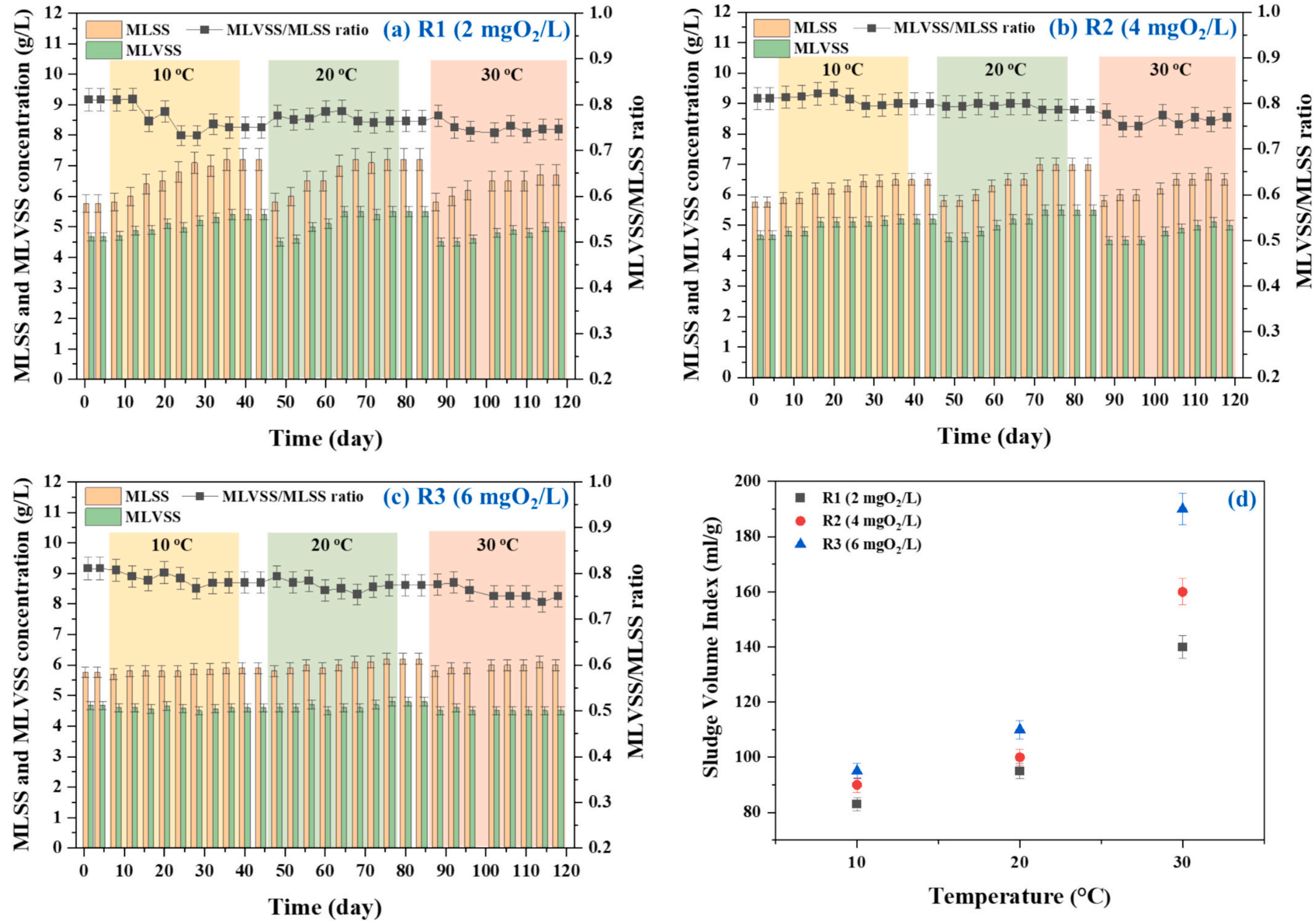

Fig. 3. Mixed liquor suspended solids (MLSS) and mixed liquor volatile suspended solids (MLVSS) concentrations, along with the MLVSS/MLSS ratio (on the secondary y-axis, right) in (a) R1 (2 mgO$_2$/L); (b) R2 (4 mgO$_2$/L); (c) R3 (6 mgO$_2$/L); and (d) sludge volume index (SVI) of the three reactors under varying temperature conditions.

accompanied by a reduction in the MLVSS/MLSS ratio, indicating an increase in non-volatile solids or less active biomass. Despite this reduction, the MLVSS/MLSS ratio remained relatively stable at around 0.75 across all reactors by the end of each operational phase, indicating consistent proportions of volatile biomass regardless of temperature or DO variations. Conversely, in R3, the growth of both MLSS and MLVSS was minimal, likely due to poor sludge floc formation, as indicated by the highest SVI in all temperature conditions. In R2, MLSS and MLVSS exhibited steady growth of 10–21 % and 8–20 %, respectively, while maintaining an MLVSS/MLSS ratio of approximately 0.8 mostly in all temperature conditions. This suggests that 4 mgO$_2$/L provided the most favourable conditions for biomass growth, balancing volatile and non-volatile solids.

The SVI, widely applied for evaluating sludge settleability, is presented in Fig. 3d. Although SVI values can vary significantly depending on the type of wastewater, treatment technology, and operational parameters, they typically range between 50 and 150 mL/g for activated sludge systems. A high SVI value indicates poor sludge settleability, which can hinder biomass aggregation and subsequent growth [39,41]. Overall, the SVI values in all three reactors at 10 °C, and 20 °C ranged between 83 and 110 mL/g, showing good sludge settleability. Across all reactors, the SVI results revealed that increasing temperature from 10 °C to 20 °C resulted in 11–16 % increases. However, further increase to 30 °C led to more significant increase of SVI values by 47 % in R1, 60 % in R2, and 73 % in R3. This resulted in 140 mL/g in R1, 160 mL/g in R2, and 190 mL/g in R3, reflecting significantly reduced sludge settleability. This trend aligns with previous studies that suggest high temperatures can impair the function of extracellular polymeric substances (EPS), which play a critical role in bioflocculation [42,43].

3.3. Microbial community analysis

3.3.1. Microbial diversity

Table 3 summarised the number of sequences and observed operational taxonomic units (OTUs), and alpha diversity indices (ACE, Chao1, Shannon, and Simpson). ACE and Chao1 indices are indicators of species richness, while Shannon and Simpson measure species evenness. Higher ACE, Chao1, and Shannon indices indicate greater microbial diversity, whereas a lower Simpson index reflects higher diversity. Overall, under 10 °C and 30 °C conditions, no significant differences in microbial diversity were observed across the three reactors. The alpha diversity indices demonstrated relatively consistent values, falling within the range of 647.6–861.4 for ACE, 624.3–812.7 for Chao1, 3.8–4.1 for Shannon, and 0.042–0.058 for Simpson. However, at 20 °C, all reactors exhibited the highest microbial evenness and richness compared to the lower (10 °C) and higher (30 °C) temperature conditions. This suggests that at extreme temperatures, certain vulnerable or temperature-sensitive microbial species may have been reduced, resulting in decreased diversity [44]. Comparisons among the three reactors at 20 °C revealed the effects of different DO levels on microbial diversity. Among the DO conditions, 4 mg/L resulted in the lowest diversity in terms of both evenness and richness. This may be attributed to the selective

Table 3
Alpha indices for microbial diversity.

		Sequences	No. of OTUs	ACE	Chao1	Shannon	Simpson
R1	**10 °C**	62,223	729	861.4	812.7	4.1	0.048
(2 mgO$_2$/L)	**20 °C**	45,797	1137	1290.0	1231.2	4.5	0.029
	30 °C	66,951	614	655.5	631.9	3.9	0.048
R2	**10 °C**	57,090	702	816.5	771.1	4.1	0.053
(4 mgO$_2$/L)	**20 °C**	46,878	822	935.8	902.0	4.3	0.034
	30 °C	65,859	610	647.6	624.3	4.0	0.046
R3	**10 °C**	66,812	677	748.9	726.3	4.0	0.042
(6 mgO$_2$/L)	**20 °C**	64,146	1518	1753.3	1692.7	4.8	0.030
	30 °C	69,657	712	800.2	774.5	3.8	0.058

enrichment of specific bacterial species that are essential for nitrification or organic matter removal. These bacteria likely thrived under their preferred environmental conditions, becoming dominant in the system and consequently reducing overall microbial diversity [45,46].

3.3.2. Microbial composition

The relative abundances from different operational phases at the phylum and genus levels were visualised in Fig. 4. The functional bacterial communities were characterised by assigning sequence reads to known phyla, resulting in the detection of 10 major phyla. Phyla with a relative abundance of less than 1 % were grouped under 'others' in Fig. 4a. Further taxonomic analysis at the genus level was performed for a more detailed understanding of bacterial communities. Fig. 4b illustrates the top 37 bacterial genera, displaying only those with a relative abundance above 2 % in at least one sample. The remaining genera are grouped under 'Others'.

Overall, the phyla *Proteobacteria, Bacteroidetes, Actinobacteria, Firmicutes*, and *Chloroflexi* were consistently among the top four dominant phyla in all samples. The prevalence of these phyla aligns with their frequent dominance in urine MBRs and municipal activated sludge communities, owing to their vital role in wastewater treatment systems [22,47,48]. *Proteobacteria* were found as the predominant phylum in all samples except for the R2 under 10 °C. Within this phylum, the predominant classes were alpha- (α-), beta- (β-), and gamma- (γ-) *Proteobacteria*. Remarkably, across all reactors with different DO levels, the relative abundance of *Proteobacteria* phylum remained largely unchanged between 10 °C and 20 °C. However, when the temperature increased to 30 °C, *Proteobacteria* showed almost 1.3 to 1.8 times higher abundance across all reactors. This trend is consistent with reports that marine *Proteobacteria* exhibit temperature-responsive metabolic activity, producing substantially more methyl halides at 30 °C than at 15 °C during exponential growth [49]. The prevailing genera within this

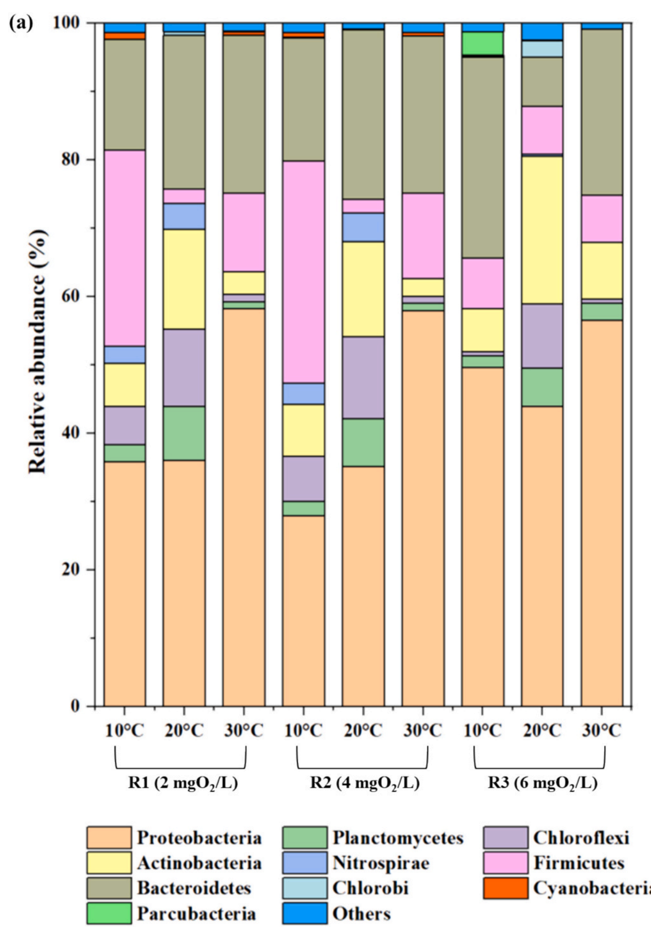

Fig. 4. Microbial community composition in terms of relative abundance (%) at (a) the phylum level; and (b) the genus level. Only phyla with relative abundance >1 % and genera with relative abundance >2 % in at least one sample are shown individually, the rest are grouped into "Others".

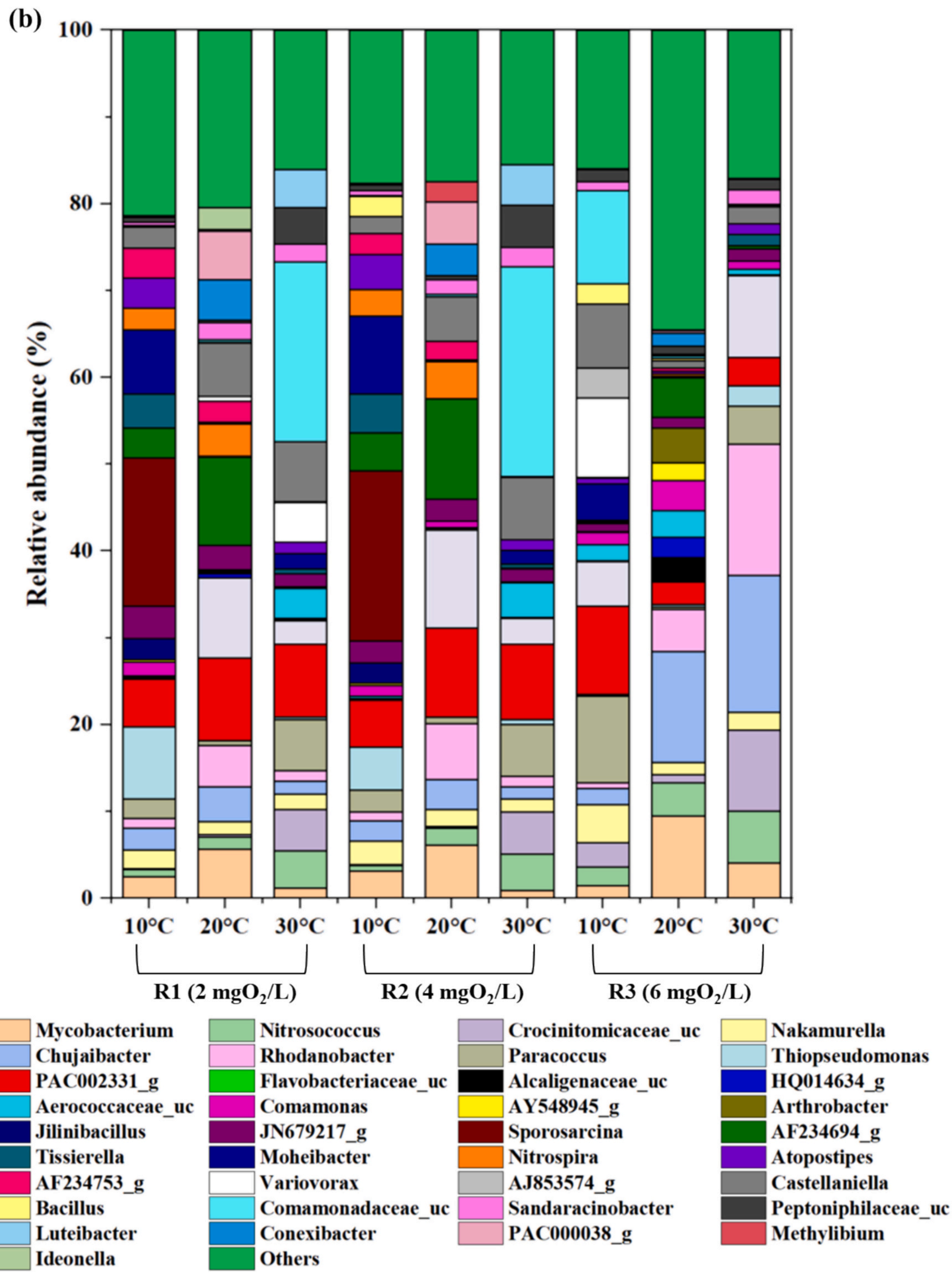

Fig. 4. (*continued*).

phylum were significantly influenced by DO conditions. Under 30 °C, both R1 and R2 were dominated by *Comamonadaceae_uc* and *Castellaniella* from the *β-Proteobacteria* class, whereas R3 was dominated by *Chujaibacter* and *Rhodanobacter* from the *γ-Proteobacteria* class. At 10 °C, *Firmicutes*, which are responsible for enzyme production for organics degradation, ranked among the top three dominant phyla across all DO conditions, showing a higher relative abundance compared to higher temperature conditions [50]. *Sporosarcina*, *Tissierella*, *Bacillus* were the predominant genera within the *Firmicutes* phylum in all reactors at 10 °C. According to the literature, *Proteobacteria*, *Firmicutes* and *Bacteroidetes* were among the most abundant groups when temperatures range between 3 °C and 16 °C. This may be attributed to the ability to resist or adapt to temperature fluctuations, allowing them to maintain their unique metabolic functions [51].

At 20 °C, significant changes in microbial composition were observed across different DO levels. In R1, the top four dominant phyla were *Proteobacteria* (36.0 %) > *Bacteroidetes* (22.5 %) > *Actinobacteria* (14.6 %) > *Chloroflexi* (11.3 %). In R2, this order remained consistent, though the relative abundances shifted slightly to 35.1 %, 24.8 %, 13.9 %, and 12.0 %, respectively. In contrast, in R3, the relative abundance changed significantly to *Proteobacteria* (43.9 %) > *Actinobacteria* (21.6 %) > *Chloroflexi* (9.4 %) > *Bacteroidetes* (7.2 %), driven primarily by the increased abundance of *Proteobacteria*. At the genus level, *AF234694_g*, belonging to the *Caldilineae* class and *Chloroflexi* phylum, was predominant in both R1 and R2, with relative abundances of 10.2 % and 11.6 %, respectively. *PAC002331_g* and *Flavobacteriaceae_uc,* which both belong to the *Bacteroidetes* phylum but are classed under the *Sphingobacteria* and *Flavobacteria* classes, respectively, were the second most abundant genera, with relative abundances ranging between 9.2 and 9.5 % and 10.3–11.3 % in R1 and R2. *Castellaniella (β-Proteobacteria)* was the fourth most abundant genus in Reactor 1, while *Rhodanobacter (γ-Proteobacteria)* held this position in Reactor 2, both reaching approximately 6 % abundance. *Mycobacterium*, belonging to the *Actinobacteria* phylum, was the next most abundant genus in both reactors. Meanwhile, in R3, the two most dominant genera were *Chujaibacter* (12.8 %) from the *γ-Proteobacteria* class and *Mycobacterium* (9.5 %) from the *Actinobacteria* phylum. *Proteobacteria*, *Bacteroidetes*, and *Chloroflexi* are known to play important roles in biodegradation of organic matter, as well as cell decay matters and soluble microbial products. Accordingly, their high levels of dominance across all three reactors reflect their strong contribution to TOC removal performance [52–54].

A closer examination of the nitrifying bacteria reveals that their composition was significantly influenced by both temperature and DO conditions. Fig. 5 illustrates the distribution of the nitrifying bacterial genera of AOB and NOB under different operational conditions. Across all reactors, the most dominant AOB genus under most conditions was *Nitrosococcus* from *γ-Proteobacteria* class, reflecting the high salinity of feed urine compared to the municipal wastewater, since *Nitrosococcus* is known to thrive in saline aquatic environments [55–58]. Additionally, *Nitrosomonas* from the *β-Proteobacteria* class was detected, showing particular dominance under 10 °C condition in R1 and R2. For NOB genera, *Nitrospira* from the *Nitrospirae* phylum was predominant, with *Nitrobacter* from the *α-Proteobacteria* class also being detected. Firstly, considering the effect of temperature on AOB genera, at the low temperature of 10 °C in R1 and R2, *Nitrosomonas* was enriched as the predominant AOB genus, reaching relative abundances of 0.9 % and 1.2 %, respectively. This predominance of *Nitrosomonas* over *Nitrosococcus* under low-temperature conditions is consistent with the findings from the previous study [59]. However, in R3 at 10 °C, while *Nitrosomonas* showed an abundance of 0.9 %, *Nitrosococcus* was the dominant genus, with a relative abundance of 2.1 %. Additionally, in all three reactors, an increase in temperature from 10 °C to 20 °C resulted in approximately double the abundance of AOB, while a further increase to 30 °C also led to an increase of 1.6–3.3 times. Meanwhile, regardless of DO conditions, the NOB genus *Nitrospira* exhibited a lower abundance at 10 °C, peaked at 20 °C, and then declined to its lowest abundance at 30 °C. As a result, *Nitrosococcus* became more abundant than *Nitrospira* at 30 °C, leading to the nitrite accumulation. This suggests that the temperature had a more significant impact on AOB growth than DO concentration, as growth rate of AOB increases at elevated temperatures. The highest level of nitrite accumulation observed in R3 at 30 °C further influenced the NOB community structure, allowing *Nitrobacter* to replace *Nitrospira* as the dominant genus. This shift likely occurred because Nitrobacter favours high-nitrite environments for its enrichment [60].

Considering the effects of DO levels, *Nitrospira* was more abundant than AOB in R1 and R2 at 10 °C and 20 °C, indicating the stable nitrification. It has been reported that *Nitrospira* has higher oxygen affinity compared to AOB, allowing it to efficiently survive in low oxygen environments, which aligns with the findings in this study [35,61]. Furthermore, Nitrospira has frequently been reported as the dominant NOB genus in nitrifying MBRs [22,62], particularly under conditions of elevated ammonium concentrations (>20 mg/L) and acidic pH, both of which align with the operational conditions applied in this study [63]. Regarding the NOB-to-AOB ratio during stable nitrification, previous studies have reported typical values ranging between 1.3 and 5.9 during stable nitrification, likely due to NOB exhibiting higher substrate uptake rates compared to AOB [64–66]. In this study, the NOB-to-AOB ratios were 1.4 and 2.8 in R1 at 10 °C and 20 °C, respectively, and 1.7 and 2.1 in R2 at the corresponding temperatures, further demonstrating the stable nitrification without nitrite accumulation. A previous urine-treating MBR operated at room temperature with a DO concentration of 4.5 mg/L similarly achieved a high NOB:AOB ratio of approximately 3.5 under steady-state conditions [22]. The increased NOB abundance observed at 20 °C was associated with reduced HRT, decreasing from an average of 16 to 12 days in R1 and from 11 to 8 days in R2 as the temperature increased from 10 °C to 20 °C. This observation is consistent with a recent study reporting that an increase in the NOB:AOB ratio from 2.9 to 5.1 was associated with a reduction in HRT to as low as ~12 h in an MBR treating nutrient-rich liquid anaerobic digestate, where *Nitrospira* was also the dominant NOB genus [62]. On the other hand, in R3, with the highest DO level, AOB exhibited a higher abundance at all temperature conditions compared to R1 and R2 with lower DO levels. These results are consistent with previous studies, which reported that AOB have a higher growth rate at elevated temperatures and DO level

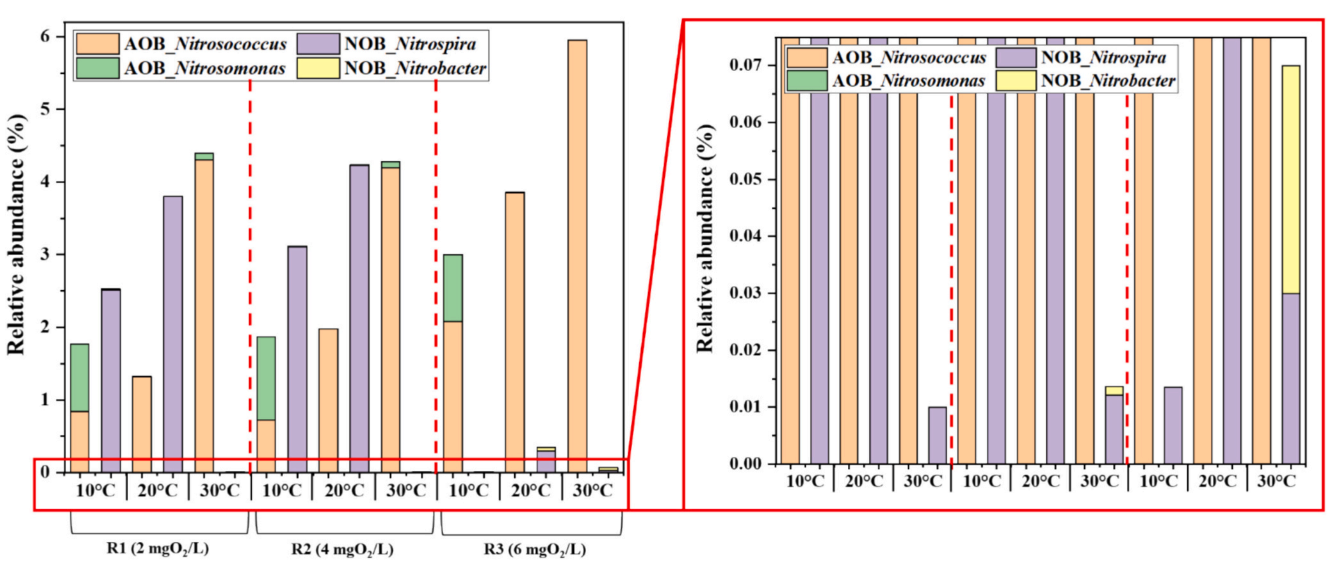

Fig. 5. Relative abundances of ammonia-oxidising bacteria (AOB) genera (Nitrosococcus and Nitrosomonas) and nitrite-oxidising bacteria (NOB) genera (Nitrospira and Nitrobacter).

compared to NOB, enabling them to rapidly dominate under favourable environmental conditions [12,33,35]. However, this imbalance was accompanied by persistent nitrite accumulation, which elevated FNA concentrations. While FNA strongly inhibited NOB activity and growth, it also reduced the activity of AOB, thereby slowing the ammonia oxidation process. Consequently, HRTs were substantially prolonged in R3, reaching an average of up to 32 days at 30 °C. This observation is consistent with previous reports describing partial inactivation of AOB under FNA stress [67].

4. Conclusions

This study investigated the effects of three temperature and DO conditions on the performance of urine-treating MBRs, in terms of nitrification rate, TOC removal, biomass growth, as well as microbial diversity and composition. The results indicated that a DO concentration of 4 mg/L at 20 °C provided optimal conditions, achieving the highest nitrification rate at 201 ± 49 mgN/L·d and the shortest HRT of approximately 8 days. This was attributed to a well-balanced abundance of AOB, specifically *Nitrosococcus*, and NOB, *Nitrospira*. In contrast, low temperature enriched *Nitrosomonas* over *Nitrosococcus*, while higher temperatures and elevated DO concentrations promoted significant enrichment of *Nitrosococcus*, due to its higher growth rate, resulting their dominance relative to NOB. These findings provide concrete guidance for optimising urine-treating MBRs by identifying operational conditions that maximise nitrification efficiency and minimise HRT, and by elucidating how temperature and DO influence the dominance of key microbial groups. These insights enable targeted strategies to enhance system performance, energy efficiency, and the reliable production of liquid fertiliser from source-separated urine. Future studies should include long-term and pilot-scale investigations to confirm the practical applicability and robustness of optimised urine-treating MBR systems.

CRediT authorship contribution statement

Weonjung Sohn: Writing – original draft, Visualization, Methodology, Investigation, Formal analysis, Data curation, Conceptualization. **Andrea Merenda:** Writing – review & editing, Formal analysis, Data curation. **A.H. Shafaghat:** Writing – review & editing, Data curation. **Ibrahim El Saliby:** Formal analysis, Data curation. **Ying Zhang:** Writing – review & editing. **Xiaodong Jia:** Writing – review & editing. **Jing Guan:** Writing – review & editing. **Sherub Phuntsho:** Writing – review & editing, Supervision, Project administration, Conceptualization. **Ho Kyong Shon:** Writing – review & editing, Supervision, Project administration, Methodology, Funding acquisition, Data curation, Conceptualization.

Declaration of competing interest

The authors declare the following financial interests/personal relationships which may be considered as potential competing interests: Given his role as Associate Editor, Dr. Andrea Merenda had no involvement in the peer review of this article and had no access to information regarding its peer review. Full responsibility for the editorial process for this article was delegated to another journal editor. If there are other authors, they declare that they have no known competing financial interests or personal relationships that could have appeared to influence the work reported in this paper.

Acknowledgements

This project is supported by the Australian Research Council (ARC) through the ARC Research Hub for Nutrients in a Circular Economy (NiCE) (IH210100001).

Data availability

Data will be made available on request.

References

[1] W. Sohn, J. Jiang, S. Phuntsho, Y. Choden, V.H. Tran, H.K. Shon, Nutrients in a circular economy: role of urine separation and treatment, Desalination (2023) 116663, https://doi.org/10.1016/j.desal.2023.116663.
[2] W. Sohn, J. Jiang, S. Phuntsho, H.K. Shon, Membrane bioreactor incorporated with biofilm carriers and activated carbon for enhanced biological nitrification of urine, Desalination (2023) 117061, https://doi.org/10.1016/j.desal.2023.117061.
[3] F. Volpin, J. Jiang, I. El Saliby, M. Preire, S. Lim, M.A. Hasan Johir, J. Cho, D. S. Han, S. Phuntsho, H.K. Shon, Sanitation and dewatering of human urine via membrane bioreactor and membrane distillation and its reuse for fertigation, J. Clean. Prod. 270 (2020) 122390, https://doi.org/10.1016/j.jclepro.2020.122390.
[4] K. Im, M. Park, M.M. Kabir, W. Sohn, Y. Choo, H.K. Shon, S.Y. Nam, Human urine electrolysis for simultaneous green hydrogen and liquid fertilizer production for a circular economy: a proof of concept, Desalination 570 (2024) 117059, https://doi.org/10.1016/j.desal.2023.117059.
[5] A. Fumasoli, B. Etter, B. Sterkele, E. Morgenroth, K.M. Udert, Operating a pilot-scale nitrification/distillation plant for complete nutrient recovery from urine, Water Sci. Technol. 73 (2016) 215–222.
[6] C. Lin, Y. Liu, Y.-Y. Li, J. Liu, Difference of high-salinity-induced inhibition of ammonia-oxidising bacteria and nitrite-oxidising bacteria and its applications, Bioresour. Technol. 387 (2023) 129640, https://doi.org/10.1016/j.biortech.2023.129640.
[7] Z. Zuo, Y. Chen, Y. Xing, S. Li, S. Yang, G. Jiang, T. Liu, M. Zheng, X. Huang, Y. Liu, The advantage of a two-stage nitrification method for fertilizer recovery from human urine, Water Res. 235 (2023) 119932, https://doi.org/10.1016/j.watres.2023.119932.
[8] Z. Zuo, T. Liu, M. Zheng, Y. Xing, D. Ren, H. Li, S. Yang, Y. Liu, Z. Yuan, X. Huang, Recovery of ammonium nitrate solution from urine wastewater via novel free nitrous acid (FNA)-mediated two-stage processes, Chem. Eng. J. 440 (2022) 135826, https://doi.org/10.1016/j.cej.2022.135826.
[9] L. Peng, H. Qiu, S. Li, Y. Xu, C. Liang, N. Wang, Y. Liu, B.-J. Ni, The mitigation effect of free ammonia and free nitrous acid on nitrous oxide production from the full-nitrification and partial-nitritation systems, Bioresour. Technol. 372 (2023) 128564, https://doi.org/10.1016/j.biortech.2022.128564.
[10] J. Jiang, S. Phuntsho, N. Pathak, Q. Wang, J. Cho, H.K. Shon, Critical flux on a submerged membrane bioreactor for nitrification of source separated urine, Process. Saf. Environ. Prot. 153 (2021) 518–526, https://doi.org/10.1016/j.psep.2021.07.039.
[11] J. Ren, D. Hao, J. Jiang, S. Phuntsho, S. Freguia, B.-J. Ni, P. Dai, J. Guan, H. K. Shon, Fertiliser recovery from source-separated urine via membrane bioreactor and heat localized solar evaporation, Water Res. 207 (2021) 117810, https://doi.org/10.1016/j.watres.2021.117810.
[12] C. De Mulder, Impact of intrinsic and extrinsic parameters on the oxygen kinetic parameters of ammonia and nitrite oxidizing bacteria, LabMET Master 104 (2014).
[13] A.C. Bolsan, C.E. Hollas, H.C. Rodrigues, J.P. Cavaler, A.C. Lazaroto, N.C. Gabiatti, M. Bortoli, G. Johann, F.G. Antes, A. Kunz, T. Edwiges, M.C. De Prá, Challenges and operational strategies to achieve partial nitrification in biological wastewater treatment: a review, Int. J. Environ. Res. 18 (22) (2024), https://doi.org/10.1007/s41742-024-00572-y.
[14] R. Li, L. Yu, R. Jiang, T. Liu, Z. Li, D. Peng, Thermodynamic characteristics of nitrifiers reveal the potential NOB inhibition strategies at low temperatures, J. Clean. Prod. 483 (2024) 144255, https://doi.org/10.1016/j.jclepro.2024.144255.
[15] E. Clements, Y. Nahum, P. Pérez-Calleja, B. Kim, R. Nerenberg, Effects of temperature on nitrifying membrane-aerated biofilms: an experimental and modeling study, Water Res. 253 (2024) 121272, https://doi.org/10.1016/j.watres.2024.121272.
[16] A. Olsson, Urine Nitrification: Start-Up with High Strength Urine, 2017.
[17] T. Wang, X. Li, Q. Dan, B. Wang, H. Wang, Y. Peng, Unraveling rapid start-up and stable maintenance of partial nitrification in domestic wastewater under high dissolved oxygen, Bioresour. Technol. 418 (2025) 131989, https://doi.org/10.1016/j.biortech.2024.131989.
[18] M. Arnaldos, Y. Amerlinck, U. Rehman, T. Maere, S. Van Hoey, W. Naessens, I. Nopens, From the affinity constant to the half-saturation index: understanding conventional modeling concepts in novel wastewater treatment processes, Water Res. 70 (2015) 458–470.
[19] Y. Bian, K. Fu, W. Yang, J. Kang, Z. Li, X. Li, H. Xi, F. Qiu, Effect of different dissolved oxygen enrichment incubation conditions on the realization of partial nitrification under microaerobic condition, J Water Process Eng 63 (2024) 105481, https://doi.org/10.1016/j.jwpe.2024.105481.
[20] B. Nowka, H. Daims, E. Spieck, Comparison of oxidation kinetics of nitrite-oxidizing bacteria: nitrite availability as a key factor in niche differentiation, Appl. Environ. Microbiol. 81 (2015) 745–753.
[21] C. Duan, Q. Zhang, J. Li, W. Feng, L. Zhang, Y. Peng, Partial nitrification response to dissolved oxygen variation and aerobic starvation: kinetics and microbial community analyses, Chem. Eng. J. 481 (2024) 148621, https://doi.org/10.1016/j.cej.2024.148621.

[22] W. Sohn, J. Jiang, Z. Su, M. Zheng, Q. Wang, S. Phuntsho, H.K. Shon, Microbial community analysis of membrane bioreactor incorporated with biofilm carriers and activated carbon for nitrification of urine, Bioresour. Technol. 397 (2024) 130462.
[23] L. Wang, K. Etebari, Z. Zhao, G.H. Walter, M.J. Furlong, Differential temperature responses between *Plutella xylostella* and its specialist endo-larval parasitoid *Diadegma semiclausum*—implications for biological control, Insect Sci. 29 (2022) 855–864, https://doi.org/10.1111/1744-7917.12967.
[24] S. Pitawala, Z. Trifunovic, J.R. Steele, H.-C. Lee, N.D. Crosbie, P.J. Scales, G.J. O. Martin, Variation of the photosynthesis and respiration response of filamentous algae (Oedogonium) acclimated to averaged seasonal temperatures and light exposure levels, Algal Res. 74 (2023) 103213, https://doi.org/10.1016/j.algal.2023.103213.
[25] M. Just, B. Albert, S. Pedrini, S. Turner, K. Dixon, Hot and fast: seed ecology for restoration relevant species in the argyle region of the East Kimberley, Australia, Restor. Ecol. 32 (2024) e14201, https://doi.org/10.1111/rec.14201.
[26] J. Jiang, W. Sohn, A. Almuntashiri, S. Phuntsho, Q. Wang, S. Freguia, I. El-Saliby, H.K. Shon, Feasibility study of powdered activated carbon membrane bioreactor (PAC-MBR) for source-separated urine treatment: a comparison with MBR, Desalination 580 (2024) 117544, https://doi.org/10.1016/j.desal.2024.117544.
[27] W. Sohn, I. El Saliby, A. Merenda, S. Phuntsho, S. Freguia, J. Guan, L. Gao, S. Lee, H.K. Shon, Anthroponics: application and effects on growth of parsley, rhipsalis, coriander, and basil fed with urine fertiliser, Desalin. Water Treat. 320 (2024) 100682, https://doi.org/10.1016/j.dwt.2024.100682.
[28] V. Faust, S.E. Vlaeminck, R. Ganigué, K.M. Udert, Influence of pH on urine nitrification: community shifts of Ammonia-oxidizing Bacteria and inhibition of nitrite-oxidizing Bacteria, ACS ES&T Engineering 4 (2024) 342–353, https://doi.org/10.1021/acsestengg.3c00320.
[29] A.D. Eaton, L.S. Clesceri, E.W. Rice, A. Greenberg, Standard Methods for the Examination of Water and Wastewater, Centennial Edition, USA, 2008. ISBN 0-087553-047-8.
[30] W. Sohn, W. Guo, H.H. Ngo, L. Deng, D. Cheng, Powdered activated carbon addition for fouling control in anaerobic membrane bioreactor, Bioresour. Technol. Rep. 15 (2021) 100721.
[31] M. Chalita, Y.O. Kim, S. Park, H.-S. Oh, J.H. Cho, J. Moon, N. Baek, C. Moon, K. Lee, J. Yang, G.G. Nam, Y. Jung, S.-I. Na, M.J. Bailey, J. Chun, EzBioCloud: a genome-driven database and platform for microbiome identification and discovery, Int. J. Syst. Evol. Microbiol. 74 (2024), https://doi.org/10.1099/ijsem.0.006421.
[32] F. Wang, Y. Yang, J. Gao, X. Li, Z. Lu, X. Fan, S. Cao, Y. Liu, L.D. Tijing, H.K. Shon, J. Ren, Ultra-rapid start-up biological nitrification for nutrient recovery from source-separated urine, Water Res. 287 (2025) 124343, https://doi.org/10.1016/j.watres.2025.124343.
[33] G. Zhu, Y. Peng, B. Li, J. Guo, Q. Yang, S. Wang, Biological removal of nitrogen from wastewater, Rev. Environ. Contam. Toxicol. (2008) 159–195.
[34] J. Gabarró, R. Ganigué, F. Gich, M. Ruscalleda, M.D. Balaguer, J. Colprim, Effect of temperature on AOB activity of a partial nitritation SBR treating landfill leachate with extremely high nitrogen concentration, Bioresour. Technol. 126 (2012) 283–289, https://doi.org/10.1016/j.biortech.2012.09.011.
[35] J. Wang, J. Song, F. Yin, Y. Shen, D. Yang, W. Liu, Insight into how high dissolved oxygen favors the startup of nitritation with aerobic granules, Chemosphere 270 (2021) 128643, https://doi.org/10.1016/j.chemosphere.2020.128643.
[36] H.N.P. Vo, X.-T. Bui, H.-H. Nguyen, T.-D. Tran, K.-J. Lee, T.-T.-T. Nguyen, B.-T. Dang, M.-H. Bui, D.D. Nguyen, T.-T.-M. Ngo, Effects of dissolved oxygen concentration on the performance of sponge membrane bioreactor treating hospital wastewater, Desalin. Water Treat. 151 (2019) 128–137.
[37] F. Meng, A. Yang, G. Zhang, H. Wang, Effects of dissolved oxygen concentration on photosynthetic bacteria wastewater treatment: pollutants removal, cell growth and pigments production, Bioresour. Technol. 241 (2017) 993–997.
[38] L. Faust, H. Temmink, A. Zwijnenburg, A.J. Kemperman, H. Rijnaarts, Effect of dissolved oxygen concentration on the bioflocculation process in high loaded MBRs, Water Res. 66 (2014) 199–207.
[39] C.S. Laspidou, B.E. Rittmann, A unified theory for extracellular polymeric substances, soluble microbial products, and active and inert biomass, Water Res. 36 (2002) 2711–2720.
[40] U. Badeti, J. Jiang, S. Kumarasingham, A. Almuntashiri, N.K. Pathak, A. Chanan, S. Freguia, W.L. Ang, N. Ghaffour, H.K. Shon, S. Phuntsho, Source separation of urine and treatment: impact on energy consumption, greenhouse gas emissions, and decentralised wastewater treatment process, Desalination 583 (2024) 117633, https://doi.org/10.1016/j.desal.2024.117633.
[41] T.T. Nguyen, H.H. Ngo, W. Guo, A. Listowski, J.X. Li, Evaluation of sponge tray-membrane bioreactor (ST-MBR) for primary treated sewage effluent treatment, Bioresour. Technol. 113 (2012) 143–147, https://doi.org/10.1016/j.biortech.2011.11.132.
[42] M. Shahzad, S. Khan, P. Paul, Influence of temperature on the performance of a full-scale activated sludge process operated at varying solids retention times whilst treating municipal sewage, Water 7 (2015) 855–867, https://doi.org/10.3390/w7030855.
[43] C. Krishna, M.C.M. Van Loosdrecht, Effect of temperature on storage polymers and settleability of activated sludge, Water Res. 33 (1999) 2374–2382, https://doi.org/10.1016/S0043-1354(98)00445-X.
[44] W.-S. Shu, L.-N. Huang, Microbial diversity in extreme environments, Nat. Rev. Microbiol. 20 (2022) 219–235.
[45] H. Wang, G. Yu, W. He, C. Du, Z. Deng, D. Wang, M. Yang, E. Yang, Y. Zhou, E. H. Sanjaya, H. Chen, Enhancing autotrophic nitrogen removal with a novel dissolved oxygen-differentiated airlift internal circulation reactor: long-term operational performance and microbial characteristics, J. Environ. Manag. 296 (2021) 113271, https://doi.org/10.1016/j.jenvman.2021.113271.
[46] H. Wang, M. Yang, K. Liu, E. Yang, J. Chen, S. Wu, M. Xie, D. Wang, H. Deng, H. Chen, Insights into the synergy between functional microbes and dissolved oxygen partition in the single-stage partial nitritation-anammox granules system, Bioresour. Technol. 347 (2022) 126364, https://doi.org/10.1016/j.biortech.2021.126364.
[47] M.B. Asif, B. Ren, C. Li, T. Maqbool, X. Zhang, Z. Zhang, Powdered activated carbon–membrane bioreactor (PAC-MBR): impacts of high PAC concentration on micropollutant removal and microbial communities, Sci. Total Environ. 745 (2020) 141090.
[48] H. Chu, X. Liu, J. Ma, T. Li, H. Fan, X. Zhou, Y. Zhang, E. Li, X. Zhang, Two-stage anoxic-oxic (a/O) system for the treatment of coking wastewater: full-scale performance and microbial community analysis, Chem. Eng. J. 417 (2021) 129204, https://doi.org/10.1016/j.cej.2021.129204.
[49] M. Hirata, M. Ikeda, F. Fukuda, M. Abe, H. Sawada, S. Hashimoto, Effect of temperature on the production rates of methyl halides in cultures of marine proteobacteria, Mar. Chem. 196 (2017) 126–134, https://doi.org/10.1016/j.marchem.2017.08.012.
[50] A. Deb, K. Gurung, J. Rumky, M. Sillanpää, M. Mänttäri, M. Kallioinen, Dynamics of microbial community and their effects on membrane fouling in an anoxic-oxic gravity-driven membrane bioreactor under varying solid retention time: a pilot-scale study, Sci. Total Environ. 807 (2022) 150878, https://doi.org/10.1016/j.scitotenv.2021.150878.
[51] R. Han, D. Zhu, J. Xing, Q. Li, Y. Li, L. Chen, The effect of temperature fluctuation on the microbial diversity and community structure of rural household biogas digesters at Qinghai plateau, Arch. Microbiol. 202 (2020) 525–538.
[52] Y. Ding, Z. Liang, Z. Guo, Z. Li, X. Hou, C. Jin, The performance and microbial community identification in mesophilic and atmospheric anaerobic membrane bioreactor for municipal wastewater treatment associated with different hydraulic retention times, Water 11 (2019) 160.
[53] Z. Feng, T. Li, Y. Lin, G. Wu, Microbial communities and interactions in full-scale A2/O and MBR wastewater treatment plants, J Water Process Eng 46 (2022) 102660, https://doi.org/10.1016/j.jwpe.2022.102660.
[54] R. De Sotto, J. Ho, W. Lee, S. Bae, Discriminating activated sludge flocs from biofilm microbial communities in a novel pilot-scale reciprocation MBR using high-throughput 16S rRNA gene sequencing, J. Environ. Manag. 217 (2018) 268–277, https://doi.org/10.1016/j.jenvman.2018.03.081.
[55] Q. Li, R. Hasezawa, R. Saito, K. Okano, K. Shimizu, M. Utsumi, Abundance and diversity of nitrifying microorganisms in marine recirculating aquaculture systems, Water 14 (2022) 2744.
[56] F. Brescia, F. Sillo, E. Franchi, I. Pietrini, V. Montesano, G. Marino, M. Haworth, E. Zampieri, D. Fusini, M. Schillaci, The 'microbiome counterattack': insights on the soil and root-associated microbiome in diverse chickpea and lentil genotypes after an erratic rainfall event, Environ. Microbiol. Rep. 15 (6) (2023) 459–483.
[57] L.S.H. Lo, Z. Xu, S.S. Lee, W.K. Lau, J.-W. Qiu, H. Liu, P.-Y. Qian, J. Cheng, How elevated nitrogen load affects bacterial community structure and nitrogen cycling services in coastal water, Front. Microbiol. 13 (2022) 1062029.
[58] M. Hayatsu, K. Tago, I. Uchiyama, A. Toyoda, Y. Wang, Y. Shimomura, T. Okubo, F. Kurisu, Y. Hirono, K. Nonaka, An acid-tolerant ammonia-oxidizing γ-proteobacterium from soil, ISME J. 11 (2017) 1130–1141.
[59] M. Chen, Y. Chen, S. Dong, S. Lan, H. Zhou, Z. Tan, X. Li, Mixed nitrifying bacteria culture under different temperature dropping strategies: nitrification performance, activity, and community, Chemosphere 195 (2018) 800–809, https://doi.org/10.1016/j.chemosphere.2017.12.129.
[60] X. Gu, Y. Huang, Y. Hu, W. Huang, M. Zhang, Impact of nitrite on partial nitrification in aerobic sewage treatment reactors under mainstream conditions, J. Environ. Chem. Eng. 10 (2022) 108414, https://doi.org/10.1016/j.jece.2022.108414.
[61] Q. Dan, X. Li, F. Zhang, R. Du, J. Li, T. Wang, Q. Zhang, Y. Peng, Saturated dissolved oxygen-driven high-rate and ultrastable partial nitrification in municipal wastewater, Bioresour. Technol. 413 (2024) 131470, https://doi.org/10.1016/j.biortech.2024.131470.
[62] A. Merenda, A.H. Shafaghat, W. Sohn, D. Seccombe, S. Phuntsho, H.K. Shon, Valorisation of liquid anaerobic digestate into liquid fertilisers via membrane bioreactors: a proof-of-concept study, Water Res. 285 (2025) 124026, https://doi.org/10.1016/j.watres.2025.124026.
[63] M.-J. Mehrani, D. Sobotka, P. Kowal, S. Ciesielski, J. Makinia, The occurrence and role of Nitrospira in nitrogen removal systems, Bioresour. Technol. 303 (2020) 122936, https://doi.org/10.1016/j.biortech.2020.122936.
[64] L. Yu, Y. Wang, R. Li, R. Zhang, X. Zhang, S. Hua, D. Peng, The differential proliferation of AOB and NOB during natural nitrifier cultivation and acclimation with raw sewage as seed sludge, RSC Adv. 10 (2020) 28277–28286.
[65] Q. Yao, D.-C. Peng, Nitrite oxidizing bacteria (NOB) dominating in nitrifying community in full-scale biological nutrient removal wastewater treatment plants, AMB Express 7 (2017) 1–11.
[66] M.K. Winkler, J.P. Bassin, R. Kleerebezem, D.Y. Sorokin, M.C. van Loosdrecht, Unravelling the reasons for disproportion in the ratio of AOB and NOB in aerobic granular sludge, Appl. Microbiol. Biotechnol. 94 (2012) 1657–1666.
[67] B. Ma, L. Yang, Q. Wang, Z. Yuan, Y. Wang, Y. Peng, Inactivation and adaptation of ammonia-oxidizing bacteria and nitrite-oxidizing bacteria when exposed to free nitrous acid, Bioresour. Technol. 245 (2017) 1266–1270, https://doi.org/10.1016/j.biortech.2017.08.074.